Mass-Spectrometric Study on Ion-Molecule Reactions of CH_5^+, $C_2H_5^+$, and $C_3H_5^+$ with C_8—C_{18} *n*-Paraffins in an Ion Trap

Yuki Tanaka, Masaharu Tsuji,*,† and Yukio Nishimura†

Department of Applied Science for Electronics and Materials, Graduate School of Engineering Sciences, Kyushu University, Kasuga, Fukuoka 816-8580

†Institute of Advanced Material Study, Kyushu University, Kasuga, Fukuoka 816-8580

(Received July 6, 2000)

Chemical ionization of *n*-paraffins (C_xH_{2x+2}: x = 8—18) by the CH_5^+, $C_2H_5^+$, and $C_3H_5^+$ ions has been studied under a reactant-ion selective mode of an ion-trap type of GC/MS. In all the reactions, $(MW-1)^+ = C_xH_{2x+1}^+$ and fragment alkyl $C_yH_{2y+1}^+$ (y = 3—$x-3$) ions were observed. The dependence of the relative intensities of $C_xH_{2x+1}^+$ and $C_yH_{2y+1}^+$ on the reaction time indicated that collisional stabilization takes part in the formation of product ions. The dependence of $C_xH_{2x+1}^+$ and $C_yH_{2y+1}^+$ distributions on the reactant hydrocarbon ions and reagent chain length was examined. The reaction mechanism was discussed from the observed product-ion distributions and heats of reactions of each pathway.

The gas phase ion-molecule reactions of *n*-paraffins in a methane atmosphere have been extensively studied since the first chemical ionization (CI) mass spectrometric measurements by Field et al.[1—4] They measured CI mass spectra of *n*-paraffins (C_xH_{2x+2}: x = 8—12,16,18,20,28,44) at a medium CH_4 pressure of 1 Torr (= 133.33 Pa), where dominant reactant ions were CH_5^+ (48%), $C_2H_5^+$ (40%), and $C_3H_5^+$ (6%).[5] The spectra consisted of major $(MW-1)^+ = C_xH_{2x+1}^+$ ions and minor fragment alkyl $C_yH_{2y+1}^+$ (y = 4—$x-1$) ions with about equal intensities. In this work, x represents the number of carbons of reagent *n*-paraffin, while y stands for the number of carbons of fragment alkyl ion. Field et al.[1,2] found that the intensity of the $C_xH_{2x+1}^+$ ion was independent of the length of the normal alkane and the relative intensities of $C_yH_{2y+1}^+$ were nearly equal. Therefore, they postulated a random attack of the reactant ion along the hydrocarbon chain. Since the reactant ions have not been separated in the CI experiments of Field et al.,[1,2] the contribution of each hydrocarbon ion to the formation of $C_xH_{2x+1}^+$ and $C_yH_{2y+1}^+$ ions has not been determined.

Clow and Futrell,[6] and Gäumann et al.[7,8] have made detailed studies of ion-molecule reactions of hexane by the CH_5^+ and $C_2H_5^+$ ions at low pressures using an ion cyclotron resonance (ICR) spectrometer. In general, the CH_5^+ ion can act as a Brϕnsted acid leading to protonated $[C_xH_{2x+2}+H]^+$ ions, while the $C_2H_5^+$ ion can function not only as a Brϕnsted acid but also as a Lewis acid leading to $[C_xH_{2x+2}+H]^+$ ions by proton transfer and $[C_xH_{2x+2}-H]^+$ ions by hydride transfer, respectively:

$$CH_5^+ + C_xH_{2x+2} \rightarrow [C_xH_{2x+2}+H]^+ + CH_4, \quad (1)$$

$$C_2H_5^+ + C_xH_{2x+2} \rightarrow [C_xH_{2x+2}+H]^+ + C_2H_4, \quad (2a)$$

$$C_2H_5^+ + C_xH_{2x+2} \rightarrow [C_xH_{2x+2}-H]^+ + C_2H_6. \quad (2b)$$

The ICR results using ^{13}C or deuterium labeled reactants provided information on general formation processes of $C_xH_{2x+1}^+$ and $C_yH_{2y+1}^+$ ions by the reactions of the CH_5^+ and $C_2H_5^+$ ions with *n*-paraffins (Scheme 1).[6—9] According to the ICR studies, CH_5^+ furnishes extremely unstable carbonium ions (**2**) and (**3**) by the attack of H^+ to a C–H or C–C bond of the alkane (**1**) ; the subsequent decomposition by loss of H_2 or smaller alkane molecules yields $C_xH_{2x+1}^+$ (**4**) and various fragment alkyl $C_yH_{2y+1}^+$ ions (**5**), respectively. The $C_yH_{2y+1}^+$ ions (**5**) are also produced by loss of alkene from $C_xH_{2x+1}^+$ (**4**). On the other hand, $C_2H_5^+$ reacts exclusively as a hydride-acceptor and not as a proton donor, even though protonation channels are thermochemically allowed. Therefore, the $C_xH_{2x+1}^+$ ions (**4**) are produced by hydride transfer and the $C_yH_{2y+1}^+$ ions (**5**) are formed by loss of alkene from $C_xH_{2x+1}^+$ (**4**). Previous ICR studies by Clow and Futrell,[6] and Gäumann et al.[7,8]

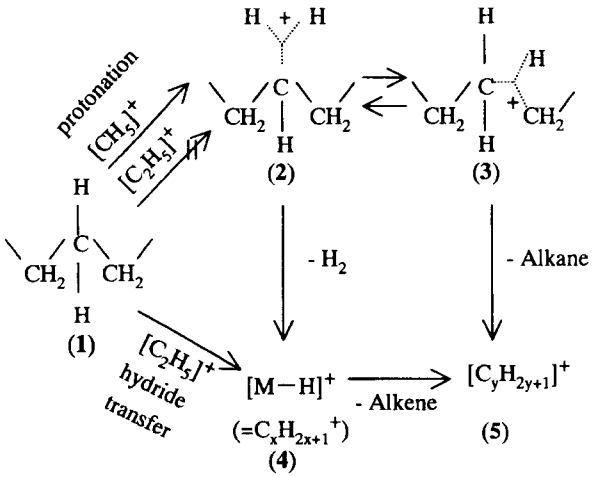

Scheme 1. Reaction scheme of ion-molecule reactions CH_5^+ and $C_2H_5^+$ with *n*-paraffins.

for *n*-paraffins have been limited to a small C_6 hydrocarbon. Therefore, the relative contribution of the reactant CH_5^+ and $C_2H_5^+$ ions to the formation of product ions (**1**), (**2**) + (**3**), (**4**), and (**5**) from larger *n*-C_xH_{2x+2} ($x = 8$—18) paraffins has not been determined.

Recently, the ion-trap detector (ITD), which can operate at much lower CI gas pressures than those in conventional medium-pressure CI mass spectrometer, has been used as a new sensitive CI mass spectrometer.[10—13] Some comparative studies between medium-pressure CI using magnetic sector instruments and low-pressure CI in the ITD have been carried out.[10—13] In general, fragmentation increases and no adduct ions such as $(M+C_2H_5)^+$ and $(M+C_3H_5)^+$ are observed in the ITD. These facts were explained by the lack of collisional stabilization of $(M+H)^+$, $(M+C_2H_5)^+$, and $(M+C_3H_5)^+$ ions due to secondary collisions with CH_4 and He gases. The other reason for the higher fragmentation in the ion-trap experiments is higher kinetic energies of reactant ions. Dorey[13] measured CH_4 CI mass spectra of *n*-$C_{14}H_{30}$ at a low CH_4 gas pressure of 10^{-5} Torr in an ITD (1 Torr $\approx$ 133.322 Pa). They found that the extent of fragmentation was much higher than that in the medium-pressure CI spectra obtained by Field et al.[1—4] Since no appreciable collisional cooling of reactant ions was found during residence times of 1—100 ms, the increased fragmentation was explained as a consequence of the high kinetic energies of reactant ions in the ITD.

Previous low-pressure CH_4 CI mass spectra of *n*-$C_{14}H_{30}$ have been measured by Dorey[13] without selecting reactant hydrocarbon ions. Therefore, the reactivity of each reactant ion for *n*-$C_{14}H_{30}$ has not been determined, as in the medium-pressure CI experiments of Field et al.[1,2] for *n*-paraffins. Although the formation mechanism of $C_xH_{2x+1}^+$ and $C_yH_{2y+1}^+$ by the reactions of CH_5^+ and $C_2H_5^+$ ions with hexane has been studied using the ICR method,[6—8] no information on the reactivity of the $C_3H_5^+$ ion for *n*-paraffins has been obtained.

In this study, CH_4 CI mass spectra of a series of *n*-paraffins (C_xH_{2x+2}: $x = 8$—18) by the CH_5^+, $C_2H_5^+$, and $C_3H_5^+$ ions are measured under a reactant-ion selective mode of an ion-trap type of GC/MS. The dependence of product-ion distributions on the reaction time was measured and compared with the previous data of Field et al.[1—4] and Dorey[13] in order to examine the effects of collisional stabilization and kinetic energies of reactant ions. The reactivity of CH_5^+, $C_2H_5^+$, and $C_3H_5^+$ for *n*-paraffins was discussed from the product-ion distributions. Preliminary results for some *n*-paraffins ($x = 14$—18) have been communicated.[14]

Experimental

CI mass spectra were obtained using an ion-trap type of Hitachi M7200 GC/MS under a reactant-ion selective mode. The electron-impact ionization on CH_4 provides primary CH_n^+ ($n = 2$—4) ions, and the subsequent fast ion-molecule reactions yield the secondary CH_5^+, $C_2H_5^+$, and $C_3H_5^+$ ions:

$$CH_4^+ + CH_4 \rightarrow CH_5^+ + CH_3 + 0.10\ \text{eV}, \quad (3)$$

$$CH_3^+ + CH_4 \rightarrow C_2H_5^+ + H_2 + 1.21\ \text{eV}, \quad (4)$$

$$CH_2^+ + CH_4 \rightarrow C_2H_3^+ + H_2 + H, \quad (5a)$$

$$C_2H_3^+ + CH_4 \rightarrow C_3H_5^+ + H_2 + 0.96\ \text{eV}. \quad (5b)$$

Here, the H° values are evaluated using reported thermochemical data.[15] Since further reactions of CH_5^+, $C_2H_5^+$, and $C_3H_5^+$ with CH_4 are very slow, these ions become dominant reactant ions in the CH_4 CI experiments. The excess energies released in reactions (3), (4), and (5b) are lower than those of the usual electronic excitation energies of molecular ions (> 3 eV), so all of the reactant ions are expected to be located in their electronic ground states. One of the reactant ions was selectively trapped as a reactant ion in an ion-trap cell. The time for storing a reactant ion was kept at a constant time of 5 ms. If reactant ions in vibrationally excited levels are formed, they will be thermalized by collisions with CH_4 and He during their trapping time in the cell. The ion-trap cell was kept at 170 °C. The reagents were diluted in hexane and injected into the GC with a high-purity carrier He gas. The partial pressures of CH_4 and He and in an ion-trap cell were 7×10^{-5} and 5×10^{-5} Torr, respectively. The reaction time corresponding to the residence time in the ion-trap was varied from 0.5 to 40 ms. The mass spectra were measured at low reagent concentrations of about 1000—10000 pg cm^{-3} in order to reduce secondary ion-molecule reactions.

The operating conditions in the ion-trap cell used in this work were significantly different from those of the conventional medium-pressure CI mass spectrometer developed by Field et al.[1—4] In the medium-pressure CI measurements, the typical CH_4 gas pressure was 1 Torr and the residence time of reactant ions in the ionization-reaction chamber was about 10 μs. Field[4] evaluated the total number of collisions of reactant ions with CH_4 during this residence time to be about 200. In the present low-pressure CI measurements, the total number of collisions of a product ion with CH_4 was estimated to be about 1—100 times within the reaction time of 0.5—40 ms from a simple gas-kinetic hard-sphere collision model. CI mass spectra were measured under the conditions where concentrations of reactant ions were much higher than those of product ions. Therefore, it was difficult to determine rate constants from plots of a decay of a reactant ion against the reaction time or the concentration of a reagent.

Results and Discussion

Contribution of Collisional Stabilization and Initial Product-Ion Distributions: When CI mass spectra resulting from ion-molecule reactions of CH_5^+, $C_2H_5^+$, and $C_3H_5^+$ with *n*-paraffins (C_xH_{2x+2}: $x = 8$—18) were measured, weak $C_xH_{2x+1}^+$ ion peaks and a number of strong fragment $C_yH_{2y+1}^+$ ion peaks were observed in most cases. If the collisional stabilization takes part in the formation of product ions, excess energy is partly relaxed by collisions with CH_4 and He gases. Then, fragmentation will be suppressed and the branching ratios of $C_xH_{2x+1}^+$ ions and large $C_yH_{2y+1}^+$ ions will be enhanced. In order to examine the contribution of collisional stabilization in our CI conditions, the dependence of product-ion distributions on the reaction time was measured. Figures 1.1, 1.2, and 1.3 show product-ion distributions of $C_xH_{2x+1}^+$ and $C_yH_{2y+1}^+$ in each reaction at five different reaction times: 0.5, 2, 10, 20, and 40 ms. In our preliminary study for *n*-paraffins (C_xH_{2x+2}: $x = 14$—18),[14] no significant reaction-time dependence was found in the product-ion distributions. However, more detailed experiments in this study demonstrated that the $C_xH_{2x+1}^+$ and $C_yH_{2y+1}^+$ distributions depend on the reaction time in most cases, though the changes

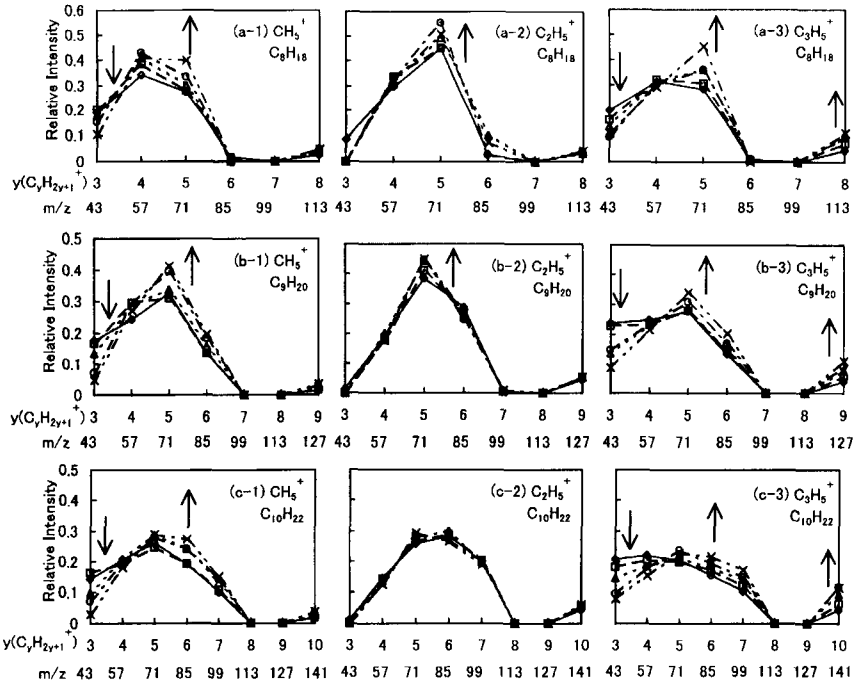

Fig. 1.1 Dependence of product-ion distributions of $C_yH_{2y+1}^+$ involving $C_xH_{2x+1}^+$ on the reaction time in the ion-molecule reactions of CH_5^+, $C_2H_5^+$, and $C_3H_5^+$ with C_8—C_{10} *n*-paraffins. Reaction time ◇: 0.5, □: 2, △: 10, ○: 20, and ×: 40 ms. Arrows indicate an increase or a decrease in product-ion distribution with an increasing the reaction time. The line connecting the points in the graphs is $C_xH_{2x+1}^+$ and $C_yH_{2y+1}^+$ formed from same reaction time.

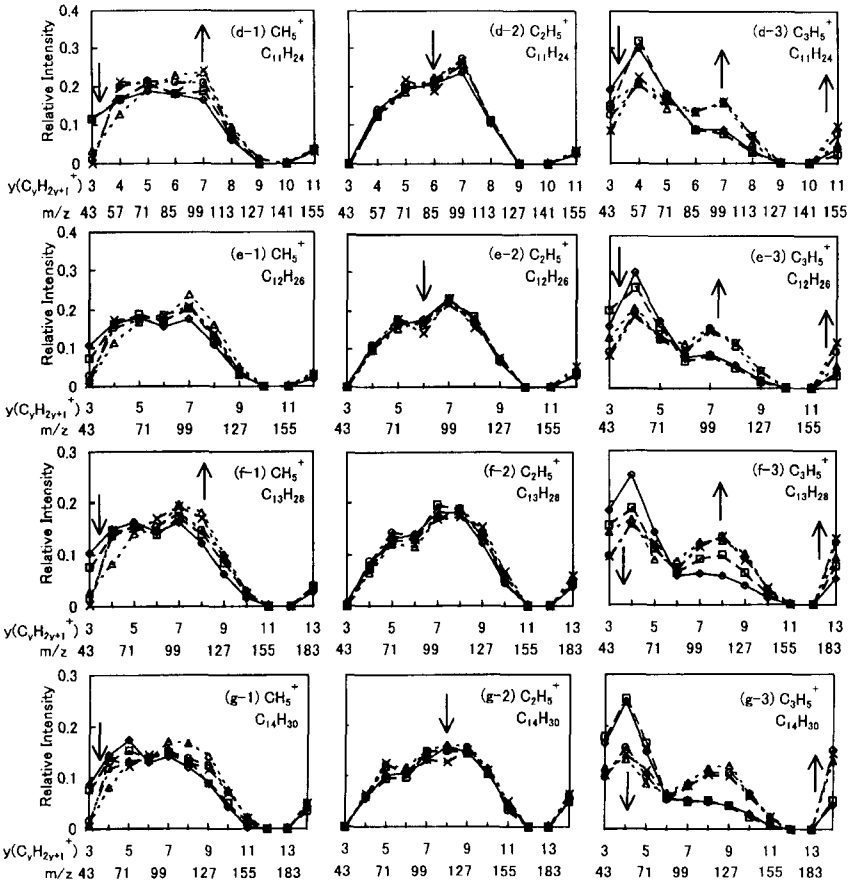

Fig. 1.2 Dependence of product-ion distributions of $C_yH_{2y+1}^+$ involving $C_xH_{2x+1}^+$ on the reaction time in the ion-molecule reactions of CH_5^+, $C_2H_5^+$, and $C_3H_5^+$ with C_{11}—C_{14} *n*-paraffins. Reaction time ◇: 0.5, □: 2, △: 10, ○: 20, and ×: 40 ms. Arrows indicate an increase or a decrease in product-ion distribution with an increasing the reaction time. The line connecting the points in the graphs is $C_xH_{2x+1}^+$ and $C_yH_{2y+1}^+$ formed from same reaction time.

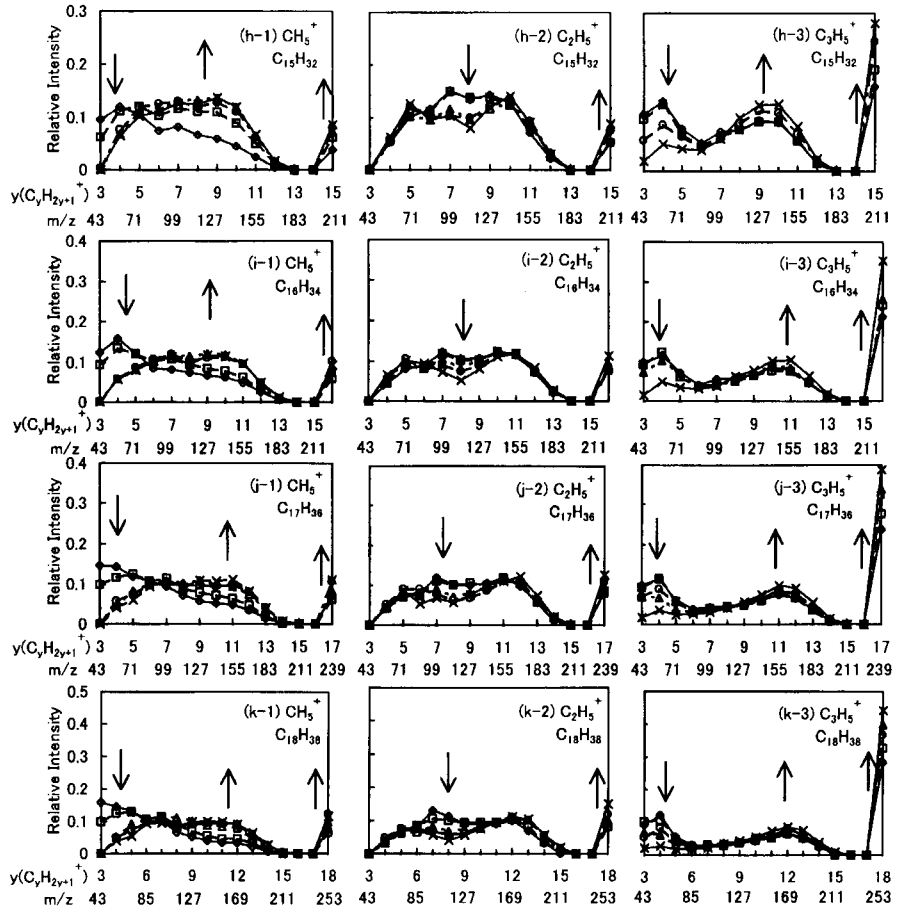

Fig. 1.3 Dependence of product-ion distributions of $C_yH_{2y+1}^+$ involving $C_xH_{2x+1}^+$ on the reaction time in the ion-molecule reactions of CH_5^+, $C_2H_5^+$, and $C_3H_5^+$ with C_{15}—C_{18} *n*-paraffins. Reaction time ◇: 0.5, □: 2, △: 10, ○: 20, and ×: 40 ms. Arrows indicate an increase or a decrease in product-ion distribution with an increasing the reaction time. The line connecting the points in the graphs is $C_xH_{2x+1}^+$ and $C_yH_{2y+1}^+$ formed from same reaction time.

in the $C_2H_5^+$ reactions are less pronounced than those in the CH_5^+ and $C_3H_5^+$ reactions. The branching ratios of almost all $C_yH_{2y+1}^+$ ions depend on the reaction time in the CH_5^+ reactions, while those of $C_yH_{2y+1}^+$ having medium y values and low y values strongly depend on the reaction time in the $C_2H_5^+$ and $C_3H_5^+$ reactions, respectively. In most cases, the branching ratios of the largest $C_xH_{2x+1}^+$ ions increase, while the small $C_yH_{2y+1}^+$ fragment ions ($y < 6$) decrease with increasing the reaction time. They are shown by arrows in Figs. 1.1, 1.2, and 1.3. On the basis of these findings, we conclude that small $C_yH_{2y+1}^+$ fragment ions result from dissociation of long-lived precursor $C_xH_{2x+1}^+$ and large $C_yH_{2y+1}^+$ ions and that these precursor ions are stabilized by secondary collisions with CH_4 and He gases at long reaction times. The initial product-ion distributions were determined by extrapolating the dependence of branching ratios of product ions on the reaction time to zero reaction time, as shown for the case of the $C_2H_5^+$/*n*-$C_{16}H_{34}$ reaction in Figs. 2(a)—(c).

Distribution of $C_yH_{2y+1}^+$: Figures 3(a)—(i) show initial product-ion distributions of $C_xH_{2x+1}^+$ and $C_yH_{2y+1}^+$ obtained for short (x = 8—10), medium (x = 11—14), and long (x = 15—18) chain reagents. The uncertainties of the initial-branching ratios were estimated to be within ±8%. The following general tendencies are observed in Figs. 3(a)—(i).

1) In the CH_5^+ reactions, the $C_yH_{2y+1}^+$ (y = 3—$x-3$) ions were observed in most cases. The intensity distribution peaks at y = 4 for the shortest chain x = 8 reagent and the maximum distribution shifts to y = 5 for x = 9—11 reagents. With increasing the carbon chain x from 12 to 14, the distributions become wider and rather flat for $y < 7$. For all the long chain x = 15—18 reagents, the distributions monotonically decrease with increasing y.

2) In the $C_2H_5^+$ reactions, the $C_yH_{2y+1}^+$ (y = 3—$x-3$) ions were observed in most cases. For short chain x = 8—10 reagents, the intensity distributions shift to high y value in comparison with those in the CH_5^+ reactions. For almost all longer chain x = 11—18 reagents, the distributions peak at y = 7 and high mass number of $C_yH_{2y+1}^+$ ions grow with increasing x. The distributions of $y < 7$ are smaller than those in the CH_5^+ reactions for all the reactions.

3) In the $C_3H_5^+$ reactions, the $C_yH_{2y+1}^+$ (y = 3—$x-3$) ions were observed in most cases. The intensity distributions of short chain x = 8—10 reagents are similar to those in the CH_5^+ reactions, though the y = 3 and 4 distributions for x = 9 and 10 are larger than those in the CH_5^+ reactions. The distributions are nearly the same for medium chain x = 11—14 reagents

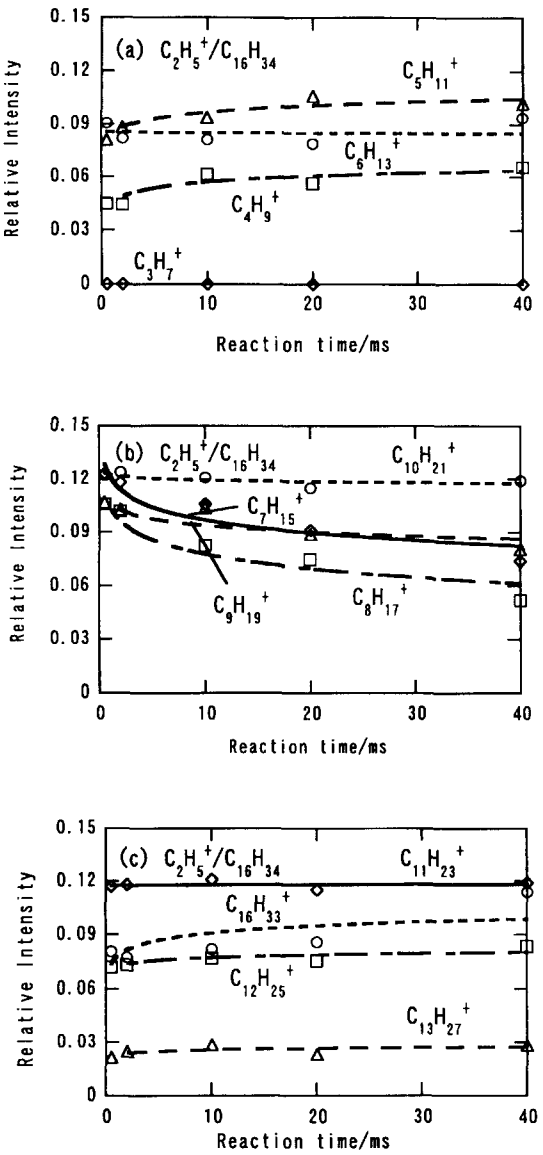

Fig. 2. Dependence of branching ratios of product ions on the reaction time in the $C_2H_5^+/n$-$C_{16}H_{34}$ reactions. (a) ◇: $C_3H_7^+$, □: $C_4H_9^+$, △: $C_5H_{11}^+$, and ○: $C_6H_{13}^+$ (b) ◇: $C_7H_{15}^+$, □: $C_8H_{17}^+$, △: $C_9H_{19}^+$, and ○: $C_{10}H_{21}^+$ (c) ◇: $C_{11}H_{23}^+$, □: $C_{12}H_{25}^+$, △: $C_{13}H_{27}^+$, and ○: $C_{16}H_{33}^+$. The lines are extrapolated to zero reaction time to find the initial product-ion distributions.

having a sharp peak at $y = 4$. The distributions of long chain $x = 15$—18 reagents are also similar to each other, here the $y = 4$ peak becomes weaker and distributions become rather flat in the $y = 6$—12 range.

Distribution of $C_xH_{2x+1}^+$ = (MW−1): Figure 4 shows the dependence of branching ratios of $C_xH_{2x+1}^+$ on the carbon chain length x in each reaction. The branching ratios of $C_xH_{2x+1}^+$ generally increase with increasing x in all the three reactions. The dependence of branching ratios of $C_xH_{2x+1}^+$ on x in the $C_2H_5^+$ reactions is similar to that in the CH_5^+ reactions, though the branching ratios in the $C_2H_5^+$ reactions are either comparable with or large in comparison with those in the CH_5^+ reactions in most cases. There is a significant difference in the branching ratios of $C_xH_{2x+1}^+$ between the $C_3H_5^+$ reactions and the CH_5^+ and $C_2H_5^+$ ones. Although the branching ratios of $C_xH_{2x+1}^+$ in the $C_3H_5^+$ reactions are small for low $x < 15$ reagents, it rapidly increases up to 30% with increasing x from 15 to 18. This may be due to a change in the responsible reaction mechanism for the formation of $C_xH_{2x+1}^+$, as discussed later.

Comparison with the Previous CI Experiments: Field et al.[1,2] measured CI mass spectra of n-paraffins (C_xH_{2x+2}: x = 8—12,16,18,20,28,44) at a medium CH_4 pressure of 1 Torr. For example, their CI mass data of n-$C_{16}H_{34}$ and n-$C_{18}H_{38}$ are shown in Figs. 5(a) and 5(b) along with our corresponding data for the $C_nH_5^+$ (n = 1—3) reactions. The CI mass spectra of Field et al.[1,2] consisted of major $(MW-1)^+ = C_xH_{2x+1}^+$ ions and minor fragment alkyl $C_yH_{2y+1}^+$ ($y = 4$ or 5—$x-1$) ions with about equal intensities, as is shown in Figs. 5(a) and 5(b). The extent of fragmentation of n-paraffins in our CI spectra was higher than that in their CI spectra. Although they observed the $C_yH_{2y+1}^+$ ($y = 4$ or 5—$x-1$) ions, the large $C_yH_{2y+1}^+$ ($y = x-2$ and $x-1$) ions could not be detected in any spectra of this study, as demonstrated in Figs. 5(a) and 5(b) for the cases of $x = 16$ and 18. They found that the variation in intensities of $C_yH_{2y+1}^+$ was quite small except for the large intensity of $C_xH_{2x+1}^+$. However, we found here that the variation in intensities of $C_yH_{2y+1}^+$ was large and that the intensity distributions of $C_yH_{2y+1}^+$ strongly depended on the reactant hydrocarbon ions. One reason for the higher extent of fragmentation observed here will be lack of collisional stabilization under our experimental conditions. The other reason will be the difference in the kinetic energy of reactant ions. The maximum and average kinetic energies of reactant ions in our apparatus were evaluated from the following relations derived from a pseudopotential well method:[16,17]

$$\overline{D}_z = \frac{eV^2}{4Z_0^2Mf^2} = \frac{6.109 \times 10^{-3}V^2}{Z_0Mf^2}, \quad (6)$$

$$E_{max} = 2e\overline{D}_z, \quad (7a)$$

$$E_{average} = \frac{8}{\pi^2}e\overline{D}_z. \quad (7b)$$

Here the depth of the pseudopotential well in the z-direction $\overline{D}_z$ is calculated in V, V is maximum a.c. voltage between the electrodes, Z_0 is half distance between end-cap electrodes in m, M is the ion mass in a.m.u., and f is the applied field frequency in MHz. In the present study the values for these parameters were $Z_0 = 0.007$, $V = 131$ (CH_5^+), 223($C_2H_5^+$), and 315($C_3H_5^+$), $f = 0.909$, and the E_{max} and $E_{average}$ values were 10 and 4.2 eV for CH_5^+, 6.0 and 2.4 eV for $C_2H_5^+$, and 4.3 and 1.7 eV for $C_3H_5^+$, respectively. These energies are higher than those in the medium-pressure CI experiments, which were estimated to be less than 1 eV.[18]

Dorey[13] measured CH_4 CI mass spectra of n-$C_{14}H_{30}$ in an ITD at residence times of 1, 10, and 100 ms without separating reactant ions. In his ITD experiment, CH_5^+ and $C_2H_5^+$ would be major reactant ions. In Figs. 6(a) and 6(b) are compared his CI spectra with the initial product-ion distributions in the reactions of CH_5^+, $C_2H_5^+$, and $C_3H_5^+$ with n-

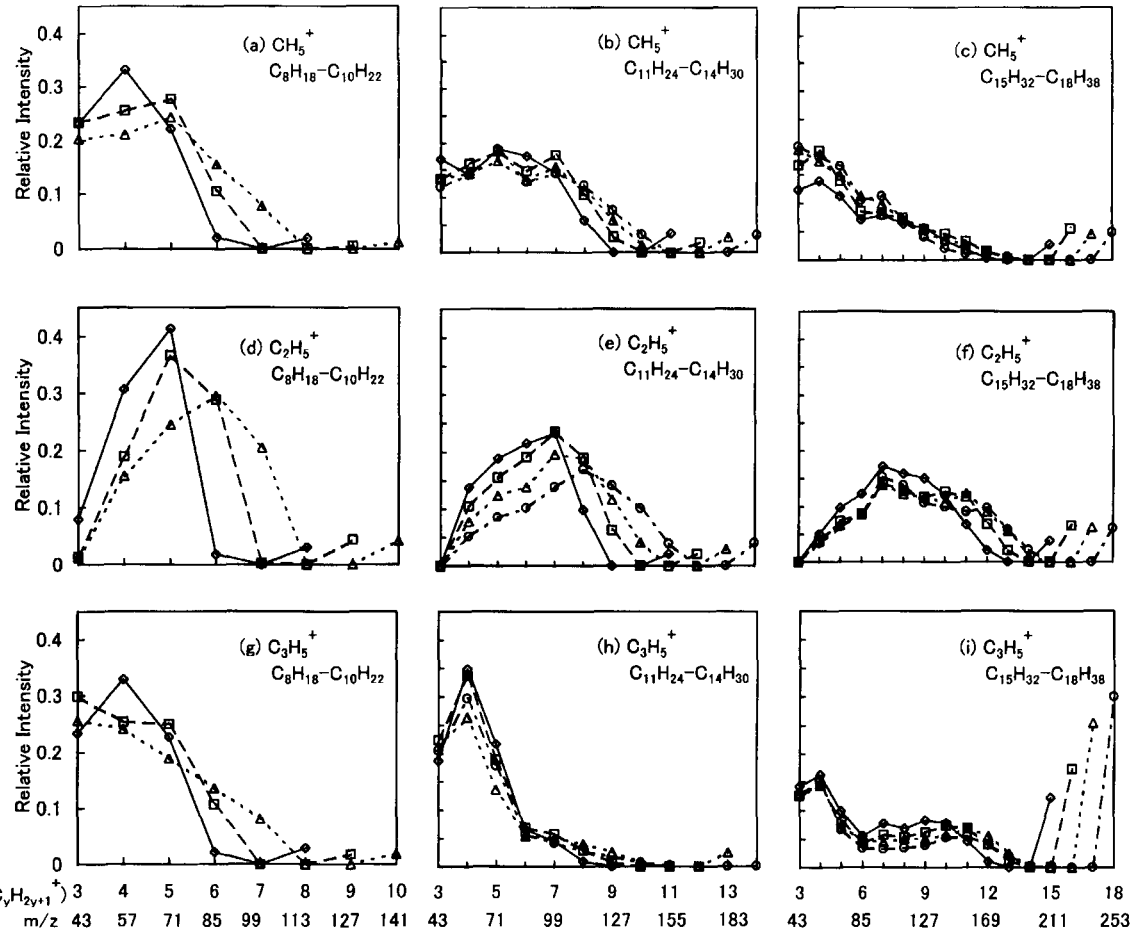

Fig. 3. Initial product-ion distributions of $C_yH_{2y+1}^+$ involving $C_xH_{2x+1}^+$ in the ion-molecule reactions of CH_5^+, $C_2H_5^+$, and $C_3H_5^+$ with C_8—C_{18} *n*-paraffins. (a),(d),(g) ◇: C_8H_{18}, □: C_9H_{20}, and △: $C_{10}H_{22}$, (b),(e),(h) ◇: $C_{11}H_{24}$, □: $C_{12}H_{26}$, △: $C_{13}H_{28}$, and ○: $C_{14}H_{30}$ (c),(f),(i) ◇: $C_{15}H_{32}$, □: $C_{16}H_{34}$, △: $C_{17}H_{36}$, and ○: $C_{18}H_{38}$. The line connecting the points in the graphs is $C_xH_{2x+1}^+$ and $C_yH_{2y+1}^+$ formed from same *n*-paraffin.

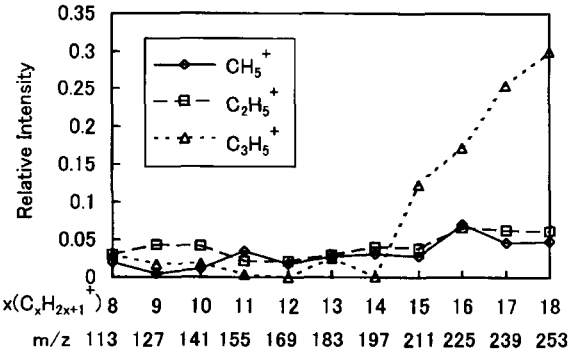

Fig. 4. Dependence of the branching ratios of $C_xH_{2x+1}^+$ on the carbon chain length x in C_xH_{2x+2}. Reactant ion ◇: CH_5^+, □: $C_2H_5^+$, and △: $C_3H_5^+$.

$C_{14}H_{30}$ obtained in this study. There are some differences in the product-ion distributions between his CI spectra and our data. The maximum distribution of $C_yH_{2y+1}^+$ ions is placed at $y = 5$ and distributions drop with increasing y in his CI spectra. On the basis of our data, the $C_yH_{2y+1}^+$ distribution in the CH_5^+ reaction also peaks at $y = 5$, though its branching ratio is smaller than that in his ITD experiment. On the other hand, the $C_yH_{2y+1}^+$ distribution in the $C_2H_5^+$ reaction peaks at $y = 8$, which is larger than that in his ITD experiment. He reported that collisional stabilization is insignificant because no appreciable change in the product-ion distributions was found during the maximum 100 ms residence time. Actually, the reaction-time dependence of distributions of $C_yH_{2y+1}^+$ is small for medium y values of 6—10 in his data. However, the branching ratio of $C_xH_{2x+1}^+$ increases and those of $C_yH_{2y+1}^+$ ($y = 4, 5$) decreases with increasing the reaction time, as shown by arrows in Fig. 6(a). These results are consistent with our present findings that the collisional stabilization participates in the formation of product ions. The lower extent of fragmentation in the CH_5^+ and $C_2H_5^+$ reactions observed in our study implies that the kinetic energies of reactant ions are lower than those in the CI experiments of Dorey.[13] Since he has not reported the detailed conditions in his ITD measurements, detailed comparison of the experimental conditions between our and his CI experiments was difficult.

Energetics and Mechanism of Each Ion-Molecule Reaction: It is known that ion-molecule reactions of CH_5^+ and $C_2H_5^+$ with *n*-paraffins provide $C_xH_{2x+1}^+$ and $C_yH_{2y+1}^+$ fragment alkyl ions. However, their relative contributions have not been determined. The most important finding in this study on the C_8—C_{18} *n*-paraffins is that not only the CH_5^+

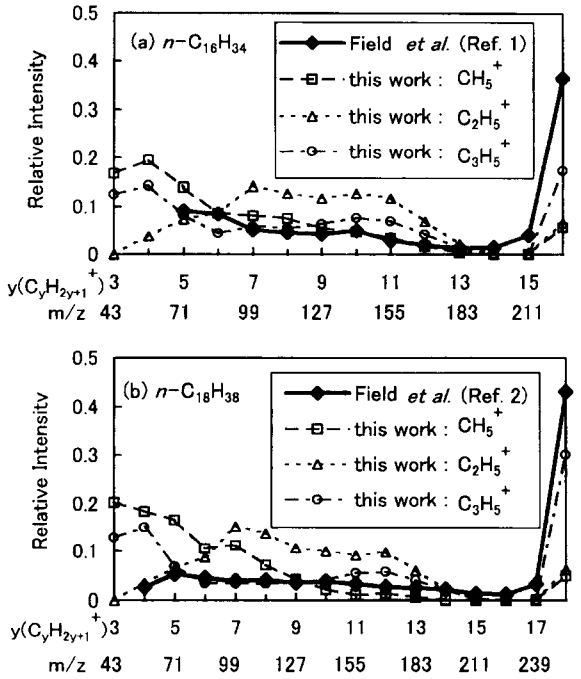

Fig. 5. CH_4 CI mass spectra of n-$C_{16}H_{34}$ and n-$C_{18}H_{38}$ obtained by Field et al. (Refs. 1, 2) in a medium-pressure without selecting reactant ions and initial distributions in the CH_5^+, $C_2H_5^+$, and $C_3H_5^+$ reactions obtained in this study. The largest $C_yH_{2y+1}^+$ ions correspond to the $C_xH_{2x+1}^+$ ions.

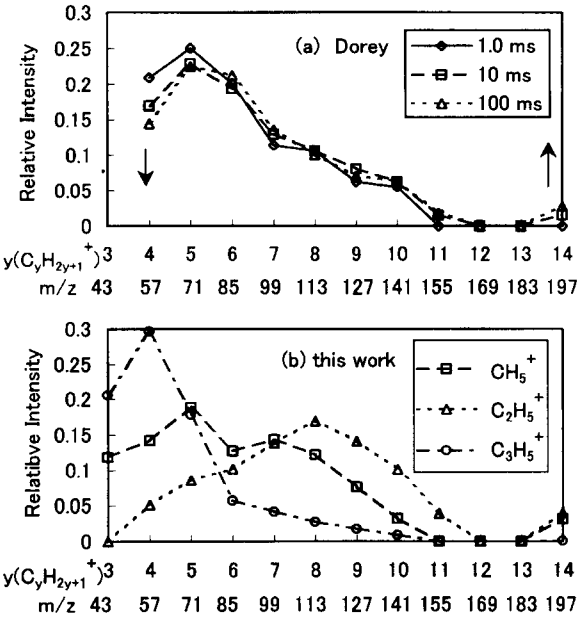

Fig. 6. CH_4 CI mass spectra of n-$C_{14}H_{30}$ obtained by Dorey (Ref. 13) in an ion trap without selecting reactant ions at various residence times and initial distributions in the CH_5^+, $C_2H_5^+$, and $C_3H_5^+$ reactions obtained in this study. Arrows indicate an increase or a decrease in product-ion distribution with an increasing the reaction time. The largest $C_yH_{2y+1}^+$ ion corresponds to the $C_xH_{2x+1}^+$ ion.

and $C_2H_5^+$ reactions but also the $C_3H_5^+$ reactions give $C_xH_{2x+1}^+$ and $C_yH_{2y+1}^+$ ions. The distributions of $C_xH_{2x+1}^+$ and $C_yH_{2y+1}^+$ were found to depend on the reactant hydrocarbon ion and on the reagent chain length.. The following two reaction pathways are possible in the ion-molecule reactions of CH_5^+ with n-paraffins leading to $C_xH_{2x+1}^+$ and $C_yH_{2y+1}^+$:

(a) Proton transfer followed by H_2 or alkane elimination:

$$CH_5^+ + C_xH_{2x+2} \rightarrow C_xH_{2x+3}^+ + CH_4, \quad (8)$$

$$C_xH_{2x+3}^+ \rightarrow C_xH_{2x+1}^+ + H_2, \quad (9a)$$

$$C_xH_{2x+3}^+ \rightarrow C_yH_{2y+1}^+ + C_{x-y}H_{2(x-y)+2}. \quad (9b)$$

(b) H^- transfer followed by alkene elimination:

$$CH_5^+ + C_xH_{2x+2} \rightarrow C_xH_{2x+1}^+ + CH_4 + H_2, \quad (10a)$$

$$C_xH_{2x+1}^+ \rightarrow C_yH_{2y+1}^+ + C_{x-y}H_{2(x-y)}. \quad (10b)$$

Although such multiple dissociation processes as $C_yH_{2y+1}^+ \rightarrow C_{y'}H_{2y'+1}^+$ ($y' < y$) + neutral hydrocarbon may also contribute to the formation of small $C_yH_{2y+1}^+$, they are excluded from the above pathways for the sake of clarity. The energetics of processes(8)—(10) was calculated using reported thermochemical data.[15] The results obtained are shown in Figs. 7(A), 7(D), and 7(G) for the cases of $x = 8$, 14, and 18 reagents. Similar energy relationships are obtained for the reactions of other n-paraffins. It is clear from Figs. 7(A), 7(D), and 7(G) that the energetics of CH_5^+ reactions is essentially independent of x of reagent. The formation of CH_3^+ is highly endoergic in all the reactions, because the heat of formation of CH_3^+ is much larger than the other $C_yH_{2y+1}^+$ ions. The ΔH values of $C_yH_{2y+1}^+ \rightarrow C_{y-1}H_{2y-1}^+ + CH_2 - 22.32$ kJ mol^{-1} are similar to those of $C_yH_{2y+1} \rightarrow C_{y-1}H_{2y-1} + CH_2 - 20.49$ kJ mol^{-1} and $C_yH_{2y} \rightarrow C_{y-1}H_{2(y-1)} + CH_2 - 20.99$ kJ mol^{-1} for $y = 2$—$x-1$.[15] Therefore, the change in the ΔH values of processes (a) and (b) is small in the $y = 2$—$x-2$ range. However, the former value is slightly larger than the latter two values, so that the ΔH values of processes (a) and (b) slightly decrease with increasing y. On the basis of the above energetics, the formation of long chain $C_yH_{2y+1}^+$ cations will be themochemically more favorable than that of long chain neutrals, if the branching ratios of $C_yH_{2y+1}^+$ are controlled thermochemically. In the CH_5^+ reactions, $C_xH_{2x+1}^+$ ion and $C_yH_{2y+1}^+$ ($y = 3$—$x-3$) ions are observed in most cases. The lack of CH_3^+ ($y = 1$) ion can be explained its high endoergicity. Although there is no significant difference in the heats of reactions for the formation of $C_2H_5^+$ and $C_3H_7^+$, the former ion is absent in all the CI experiments. This can be explained by the lack of stabilization of $C_2H_5^+$ ion by isomerization, while more stable s-$C_3H_7^+$ ions can be formed. It should be noted that processes (a) are exoergic, while processes (b) are endoergic without taking account of the formation of more stable isomers. Combining previous isotopic studies with the energetics given in Figs. 7(A), 7(D), and 7(G) led us to conclude that ion-molecule reactions of CH_5^+ with n-paraffins are controlled thermochemically, so that low energy processes (a) take place exclusively.

The following three reaction pathways are possible in the ion-molecule reactions of $C_2H_5^+$ with n-paraffins for the formation of $C_xH_{2x+1}^+$ and $C_yH_{2y+1}^+$:

(c) Proton transfer followed by H_2 and alkane elimination:

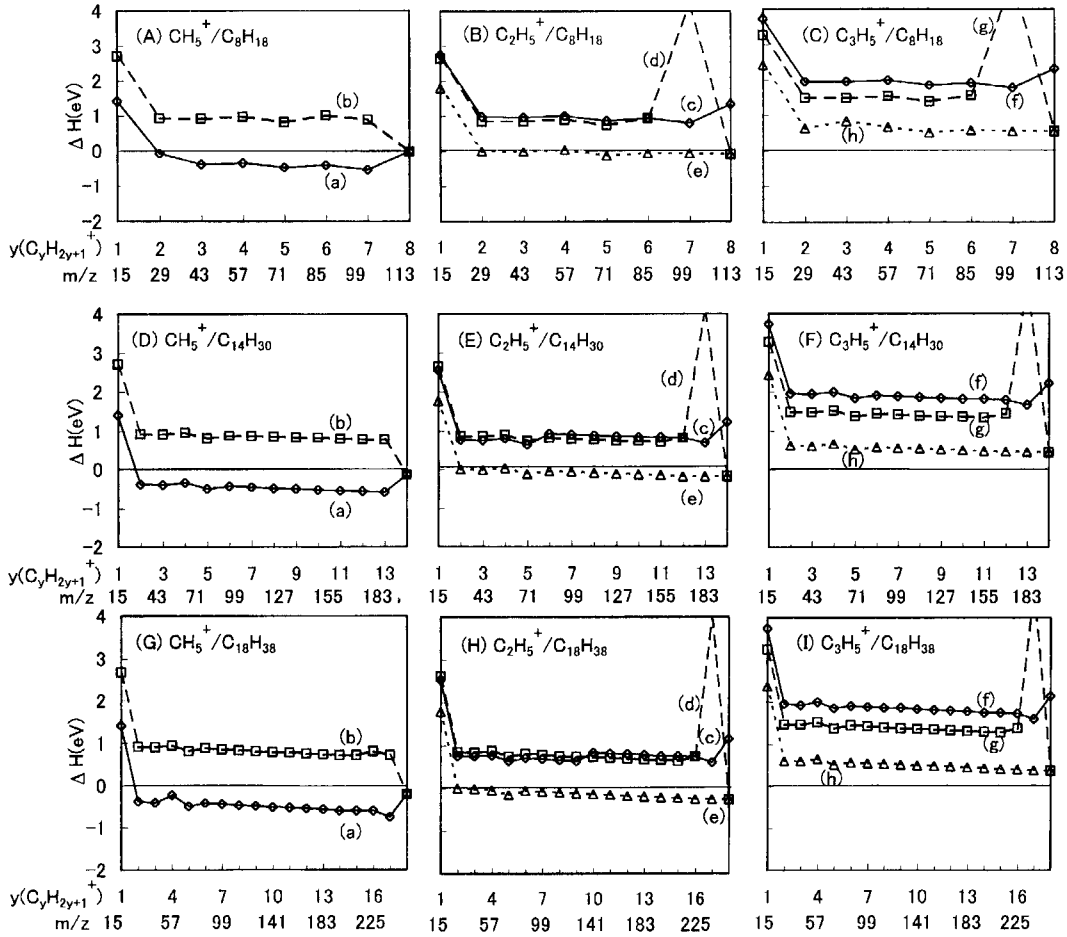

Fig. 7. Energy relations in the ion-molecule reactions of CH_5^+, $C_2H_5^+$, and $C_3H_5^+$ with n-C_8H_{18}, n-$C_{14}H_{30}$, and n-$C_{18}H_{38}$ leading to n-$C_xH_{2x+1}^+$ and n-$C_yH_{2y+1}^+$. (A),(D),(G) ◇:(a) Proton transfer followed by H_2 or alkane elimination, □: (b) H^- transfer followed by alkene elimination, (B),(E),(H) ◇: (c) Proton transfer followed by H_2 and alkane elimination, □: (d) H^- transfer followed by alkene elimination, △: (e) alkanide ion transfer followed by alkane elimination, (C),(F),(I) ◇: (f) Proton transfer followed by alkane elimination, □: (g) H^- transfer followed by alkene elimination, △: (h) alkanide ion transfer followed by alkene elimination. The largest $C_yH_{2y+1}^+$ ions correspond to the $C_xH_{2x+1}^+$ ions. The line connecting the points in the graphs is $C_xH_{2x+1}^+$ and $C_yH_{2y+1}^+$ formed from same reaction pathway.

$$C_2H_5^+ + C_xH_{2x+2} \rightarrow C_xH_{2x+3}^+ + C_2H_4, \quad (11)$$

$$C_xH_{2x+3}^+ \rightarrow C_xH_{2x+1}^+ + H_2, \quad (12a)$$

$$C_xH_{2x+3}^+ \rightarrow C_yH_{2y+1}^+ + C_{x-y}H_{2(x-y)+2}. \quad (12b)$$

(d) H^- transfer followed by alkene elimination:

$$C_2H_5^+ + C_xH_{2x+2} \rightarrow C_xH_{2x+1}^+ + C_2H_6, \quad (13a)$$

$$C_xH_{2x+1}^+ \rightarrow C_yH_{2y+1}^+ + C_{x-y}H_{2(x-y)}. \quad (13b)$$

(e) alkanide ion transfer followed by alkane elimination:

$$C_2H_5^+ + C_xH_{2x+2} \rightarrow C_yH_{2y+1}^+ + C_{x-y+2}H_{2(x-y+2)+2}. \quad (14)$$

Multiple dissociation processes such as $C_yH_{2y+1}^+ \rightarrow C_{y'}H_{2y'+1}^+$ ($y' < y$) + neutral hydrocarbon, which may be responsible for the formation of small $C_yH_{2y+1}^+$ ions, are excluded from the above pathways for the sake of clarity. The energetics of the above processes are shown in Figs. 7(B), 7(E), and 7(H) for the cases of $x = 8$, 14, and 18 reagents. Similar relationships are obtained for the reactions of other n-paraffins. In all the reactions, only processes (e) are energetically accessible for the formation of n-$C_yH_{2y+1}^+$. Previous isotopic studies on n-C_6H_{14} demonstrated that processes (d) exclusively occur. The formation of n-$C_yH_{2y+1}^+$ is endoergic. However, that of s-$C_yH_{2y+1}^+$ and t-$C_yH_{2y+1}^+$ cations will become exoergic, because ΔH values of secondary and tertiary carbocations are lower than that of primary ones by 0.87 and 1.3 eV, respectively.[2] Thus, product $C_yH_{2y+1}^+$ ions will be such more stable isomer ions in the $C_2H_5^+$ reactions. There are no significant differences in heats of reactions between processes (c) and (d) except for great differences in the formation of the large n-$C_xH_{2x+1}^+$ and $C_yH_{2y+1}^+$ ($y = x-1$) ions. Although the heats of formation of small $C_yH_{2y+1}^+$ ($y = 1$—3) ions are known, those of larger $C_yH_{2y+1}^+$ ions have not been determined probably because of the instability of $C_yH_{2y+1}^+$ ($y \geq 4$). The facts that the formation of $C_xH_{2x+1}^+$ and $C_yH_{2y+1}^+$ takes place by H^- abstraction are probably due to the facts that the heats of reactions leading to $C_xH_{2x+1}^+$ through processes (d) are smaller than those through processes (c) and that the energy barriers for the formation of unstable intermediate $C_xH_{2x+3}^+$

protonated ions are higher than those in the H^- processes.

There are three possible reaction processes in the $C_3H_5^+$ reactions, as in the cases of the $C_2H_5^+$ reactions:

(f) Proton transfer followed by alkane elimination:

$$C_3H_5^+ + C_xH_{2x+2} \rightarrow C_xH_{2x+3}^+ + C_3H_4 \quad (15)$$

$$C_xH_{2x+3}^+ \rightarrow C_xH_{2x+1}^+ + H_2, \quad (16a)$$

$$C_xH_{2x+3}^+ \rightarrow C_yH_{2y+1}^+ + C_{x-y}H_{2(x-y)+2}. \quad (16b)$$

(g) H^- transfer followed by alkene elimination:

$$C_3H_5^+ + C_xH_{2x+2} \rightarrow C_xH_{2x+1}^+ + C_3H_6, \quad (17a)$$

$$C_xH_{2x+1}^+ \rightarrow C_yH_{2y+1}^+ + C_{x-y}H_{2(x-y)}. \quad (17b)$$

(h) alkanide ion transfer followed by alkene elimination:

$$C_3H_5^+ + C_xH_{2x+2} \rightarrow C_yH_{2y+1}^+ + C_{x-y+3}H_{2(x-y+3)}. \quad (18)$$

Multiple dissociation processes such as $C_yH_{2y+1}^+ \rightarrow C_{y'}H_{2y'+1}^+$ ($y' < y$) + neutralhydrocarbon are excluded from the above processes for the sake of clarity. The energetics of the above processes leading to n-$C_yH_{2y+1}^+$ is shown in Figs. 7(C), 7(F), and 7(I) for the cases of $x = 8$, 14, and 18 reagents. There are three possible $C_3H_5^+$ isomers, whose H° values are 946, 969, and 1069 kJ mol^{-1} for CH_2=$CHCH_2^+$, CH_3C=CH_2^+, and protonated cyclopropene ion, respectively.[15] Since the most stable CH_2=$CHCH_2^+$ isomer is a significant ion produced from CH_4 CI gas,[19] all thermochemical calculations for $C_3H_5^+$ are carried out using the above H° value of CH_2=$CHCH_2^+$. Although all processes (f), (g), and (h) leading to n-$C_xH_{2x+1}^+$ are endoergic, the formation of $C_xH_{2x+1}^+$ and $C_yH_{2y+1}^+$ was found in this study. On the basis of the observed $C_yH_{2y+1}^+$ distributions, the extent of fragmentation in the $C_3H_5^+$ reactions was determinated to be higher than that in the $C_2H_5^+$ reactions for short $x = 8$—14 reagents. This indicates that more excess energies are released in the $C_3H_5^+$ reactions. Since the kinetic energies of $C_3H_5^+$ are expected to be lower than those of $C_2H_5^+$, the higher extent of fragmentation cannot be attributed to the difference in the initial kinetic energies of the reactant ions. It can be explained by assuming that $C_yH_{2y+1}^+$ ions are dominantly formed through lower-energy direct alkanide-ion transfer processes (h). It should be noted that the extent of fragmentation in the $C_3H_5^+$ reactions becomes low in comparison with that in the $C_2H_5^+$ reactions for long $x = 15$—18 reagents. This implies that dominant formation processes of $C_yH_{2y+1}^+$ ions are proton transfer (f) and/or H^- abstraction (g). On the basis of the energetics of each reaction [Figs. 7(C), 7(F), and 7(I)], the latter process is more favorable than the former process, because the formation of precursor $C_xH_{2x+1}^+$ ions through process (g) is about 1.5 eV more stable than that through process (f). Therefore, it will be the dominant pathway for $x = 15$—18 reagents. The change in dominant process from (h) to (g) for long chain reagents cannot be explained from the heats of reactions, because the energy relationships leading to $C_yH_{2y+1}^+$ are similar for all the reagents ($x = 8$—18), as shown in Figs. 7(C), 7(F), and 7(I). It may arise from a difference in the energy barrier in entrance channels, which depends on chain length. Further detailed theoretical studies on energy barriers are required to explain why such a drastic change in reaction mechanism occurs between $x = 8$—14 and $x = 15$—18 in the $C_3H_5^+$ reactions.

Concluding remarks: The gas-phase ion-molecule reactions of CH_5^+, $C_2H_5^+$, and $C_3H_5^+$ with n-paraffins (C_xH_{2x+2}: $x = 8$—18) have been studied under a reactant-ion selective chemical ionization mode of an ion-trap type of GC/MS. In all the reactions, $(MW-1)^+ = C_xH_{2x+1}^+$ and fragment alkyl $C_yH_{2y+1}^+$ ($y = 3$—$x-3$) ions were observed. The dependence of the relative intensities of $C_xH_{2x+1}^+$ and $C_yH_{2y+1}^+$ on the reaction times indicated that collisional stabilization takes part in the formation of product ions and that small $C_yH_{2y+1}^+$ ions arise from decomposition of $C_xH_{2x+1}^+$ and large $C_yH_{2y+1}^+$. The branching ratios of $C_xH_{2x+1}^+$ generally increased with increasing carbon chain length x. The $C_xH_{2x+1}^+$ and $C_yH_{2y+1}^+$ distributions depended strongly on the reactant hydrocarbon ions and reagent chain length. Although the extent of fragmentation in the $C_3H_5^+$ reactions was higher for short chain $x < 15$ reagents than that in the $C_2H_5^+$ reactions, it was lower than that in the $C_2H_5^+$ reactions for long chain $x > 14$ reagents. This was explained as a consequence of reaction change from direct alkanide ion abstraction to hydride abstraction, though further detailed studies including isotopic studies are required in order to confirm this prediction.

The authors acknowledge financial support from the Mitsubishi Foundation and a Grant-in-Aid for Scientific Research No. 09440201 from the Ministry of Education, Science, Sports and Culture.

References

1 M. S. B. Munson and F. H. Field, *J. Am. Chem. Soc.*, **88**, 2621 (1966).

2 F. H. Field, M. S. B. Munson, and D. A. Becker, "Advances in Chemistry Series," No. **58**, *Am. Chem. Soc.*, Washington, D.C. (1966), pp. 167—192.

3 F. H. Field, *Acc. Chem. Res.*, **1**, 42 (1968).

4 F. H. Field, in "Mass Spectrometry, MTP Intern. Rev. Sci., Phys. Chem. Ser. 1," Vol. 5, ed. by Maccoll, Butterworths (1972), pp. 133—181.

5 M. S. B. Munson and F. H. Field, *J. Am. Chem. Soc.*, **89**, 1047 (1968).

6 R. P. Clow and J. H. Futrell, *J. Am. Chem. Soc.*, **94**, 3748 (1972).

7 R. Houriet, G. Parsod, and T. Gäumann, *J. Am. Chem. Soc.*, **99**, 3599 (1977).

8 R. Houriet and T. Gäumann, *Int. J. Mass Spectrom. Ion Phys.*, **28**, 93 (1978).

9 W. J. Richter and H. Schwartz, *Angew. Chem., Int. Ed. Engl.*, **17**, 424 (1978).

10 R. E. Mather and J. F. J. Todd, *Int. J. Mass Spectrom. Ion Process.*, **30**, 1 (1979).

11 J. S. Brodbelt, J. N. Louris, and R. G. Cooks, *Anal. Chem.*, **59**, 1278 (1987).

12 S. M. Boswell, R. E. Mather, and J. F. J. Todd, *Int. J. Mass Spectrom. Ion Process.*, **99**, 139 (1990).

13 R. C. Dorey, *Org. Mass Spectrom.*, **24**, 973 (1989).

14 M. Tsuji, Y. Tanaka, T. Arikawa, and Y. Nishimura, *Chem. Lett.*, **1999**, 1281.

15 S. G. Lias, J. E. Bartmess, J. F. Liebman, J. L. Holmes, R. D. Levin, and W. G. Mallard, *J. Phys. Chem. Ref. Data*, **17**, Suppl. 1 (1988); Updated data were obtained from NIST Standard Ref. Database, Number 69, 2000, (http://webbook.nist.gov/chemistry).

16 H. G. Dehmelt, *Adv. Atom. Mol. Phys.*, **3**, 53 (1967); **5**, 109, (1969).

17 J. F. J. Todd, R. M. Waldren, and R. F. Bonner, *Int. J. Mass Spectrom. Ion Phys.*, **34**, 17 (1980).

18 C. Chang, G. G. Meisels, and J. A. Taylor, *Int. J. Mass Spectrom. Ion Phys.*, **12**, 411 (1973).

19 R. Houriet, T. A. Elwood, and J. H. Futrell, *J. Am. Chem. Soc.*, **100**, 2320 (1978).